CORROSION SCIENCE AND TECHNOLOGY, Vol.9, No.6(2010), pp.281~288

Carbon Corrosion at Pt/C Interface in Proton Exchange Membrane Fuel Cell Environment

Min-Ho Choi, Won-Jin Beom, and Chan-Jin Park†

Department of Materials Science and Engineering, Chonnam National University, 77, Yongbong-ro, Buk-gu, Gwangju 500-757, Korea
(Received October 15, 2009; Revised December 10, 2010; Accepted December 13, 2010)

This study examined the carbon corrosion at Pt/C interface in proton exchange membrane fuel cell environment. The Pt nano particles were electrodeposited on carbon substrate, and then the corrosion behavior of the carbon electrode was examined. The carbon electrodes with Pt nano electrodeposits exhibited the higher oxidation rate and lower oxidation overpotential compared with that of the electrode without Pt. This phenomenon was more active at 75 ℃ than 25 ℃. In addition, the current transients and the corresponding power spectral density (PSD) of the carbon electrodes with Pt nano electrodeposits were much higher than those of the electrode without Pt. The carbon corrosion at Pt/C interface was highly accelerated by Pt nano electrodeposits. Furthermore, the polarization and power density curves of PEMFC showed degradation in the performance due to a deterioration of cathode catalyst material and Pt dissolution.

Keywords *: carbon corrosion, Pt particle, oxidation, overpotential*

1. Introduction

After a long operation of proton exchange membrane fuel cell (PEMFC), its performance has become degraded due to the loss of Pt catalysts by the corrosion of carbon support.[1),2)] In particular, the carbon corrosion can be accelerated by the repeated shutdown and re-start of PEMFC. When restarting PEMFC, air can still be remained near anode and water near cathode. This phenomenon may induce the condition of "fuel starvation" in anode. The potentials of both electrodes increase, and accordingly the corrosion of carbon support in cathode can occur.[2)] In addition, it has been reported that Pt catalysts accelerates the corrosion of carbon support.[2)] In addition, it is not easy to observe directly the carbon corrosion in operating PEMFC. In this study, we investigated the carbon corrosion at Pt/C interface in a PEMFC environment.

2. Experimental

The working electrodes for experiments were prepared by electrodepositing Pt on the carbon electrode supplied by Dongbang carbon Co., Ltd. in a solution of 5 mM H_2PtCl_6 and 0.5 M H_2SO_4 using pulse deposition technique.[3),4)] The electrochemical cell is composed of a carbon electrode as a working electrode, a Pt wire as a counter electrode and a saturated calomel electrode (SCE) as a reference electrode. The applied potential for Pt electrodeposition ranges from 0.4 ~ 1.0 V_{NHE}. The size and density of Pt electrodeposits were controlled by varying electrodeposition time from 5 to 30 s. We analyzed the cyclic voltammograms for the carbon electrodes in 0.5 M H_2SO_4 solution at 25 ℃ and 75 ℃, respectively. In addition, the potentiostatic current transients for the electrodes were measured with increasing applied potential. Then, the current transients were analyzed in frequency domain using maximum entropy method (MEM).[5)-7)] For microstructural analysis, we used a scanning electron microcopy (SEM).

A single fuel cell was tested using a test fixture with a 25 cm^2 apparent area. The fixture was composed of a pair of graphite plates with serpentine flow fields for the reactants. Polarization and power density curves were obtained using a PEMFC test station obtained from CNL Energy Inc. in galvanostatic polarization mode. It is necessary to activate the membrane electrodes assembly (MEA, 3M Inc.) before the tests to ensure that the electrolyte in MEA and electrode were moist enough to have high ionic conductivity. Hydrogen and air were used as the reactants at ambient pressure with a flow rate of 1480 and 466 $cc \cdot min^{-1}$ across the anode and cathode, respectively. Both re-

† Corresponding author: parkcj@chonnam.ac.kr

actants were 100% humidified by passing them through humidifiers before entering the cell. The cell temperature was maintained at 70 ℃ with the H_2 and Air gases humidified at 75 ℃. The operation was carried out at a constant current density from 0 A·cm^{-2} to 20 A·cm^{-2} at a step interval of 0.5 A·cm^{-2}. In addition, the PEMFC had been operated for 8 h and stopped for remnant 16 h. Thus, 1 cycle for test was composed of 8 h operation and 16 h rest time.

After the electrochemical tests, the MEA was removed carefully from the cell. The anode and cathode gas diffusion layers (GDLs) were separated from the MEA and cut into smaller pieces for subsequent analysis by SEM, XRD and EDS. The new MEA was also characterized using the same techniques for comparison.

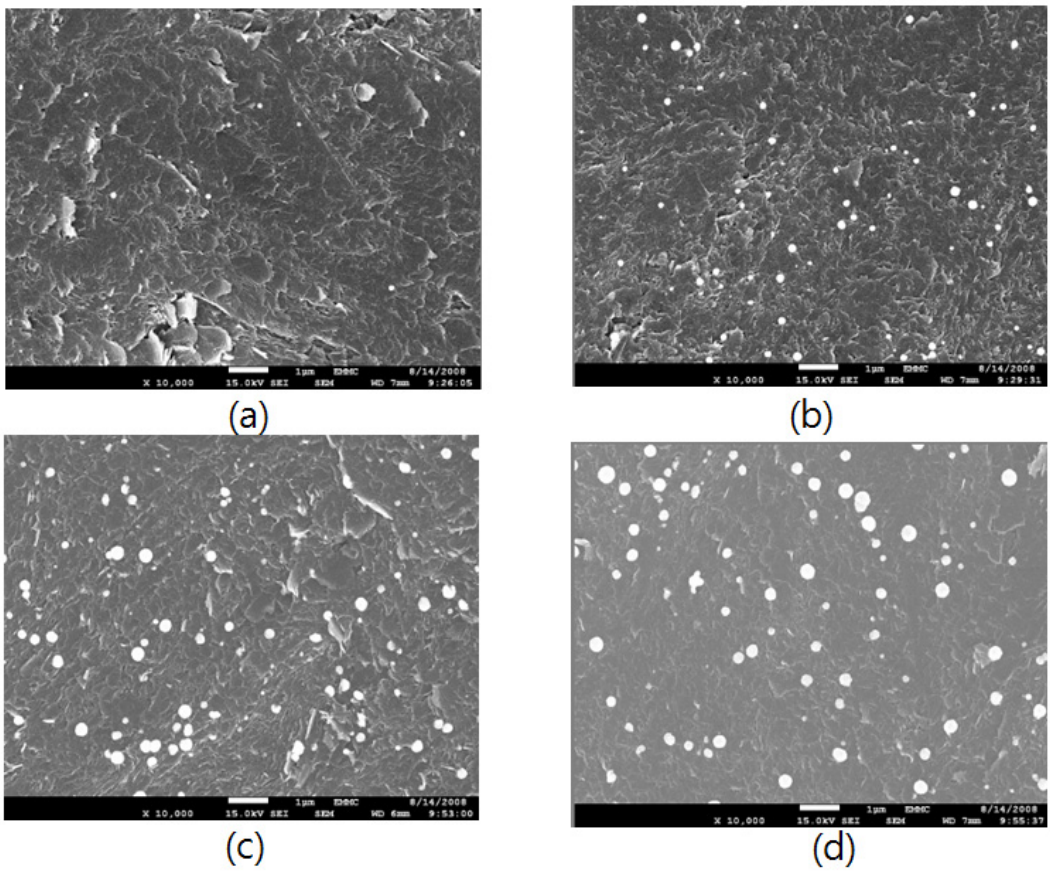

Fig. 1. SEM micrographs of Pt nano particles electrodeposited for (a) 5 s, (b) 10 s, (c) 20 s, and (c) 30s.

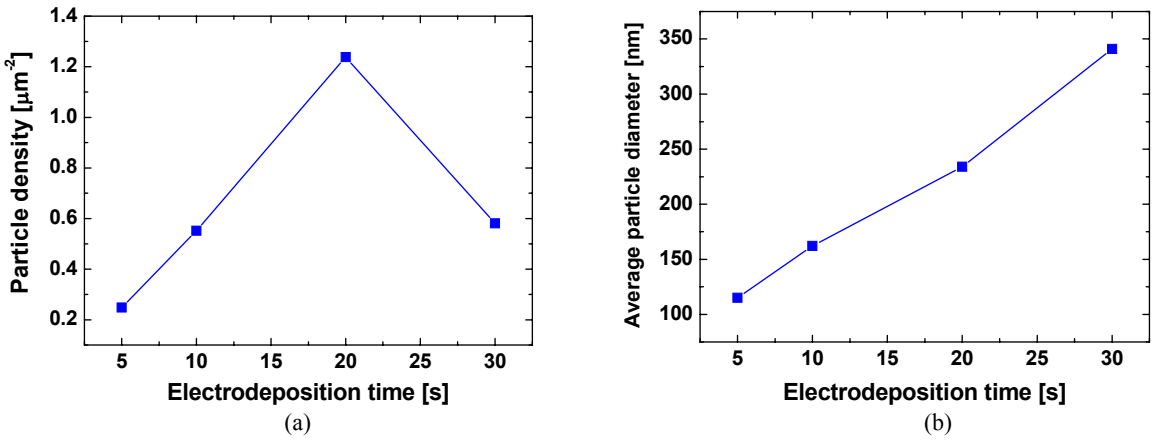

Fig. 2. Density and average size of Pt nano electrodeposits as a function of electrodeposition time (5 ~ 30 s).

3. Results and discussion

3.1 Electrode fabrication by pulse electrodeposition method

Fig. 1 and 2 show the SEM images and the density and average size of Pt nano particles electrodeposited on carbon substrate, respectively, as a function of deposition time. With increasing electodeposition time from 5 to 30 s, the density of the Pt electrodeposits increased up to 20 s and then decreased to reduce surface energy, while the diameter of the electrodeposits increased gradually from 100 to 350 nm.

3.2 Cyclic voltammograms of the carbon electrodes

Fig. 3 shows the effect of electrodeposition time (0 ~ 20s) on the cyclic voltammograms of carbon electrodes in 0.5 M H_2SO_4 solution at 25 ℃ and 75 ℃, respectively. At 25 ℃, on the whole, anodic current for the electrodes

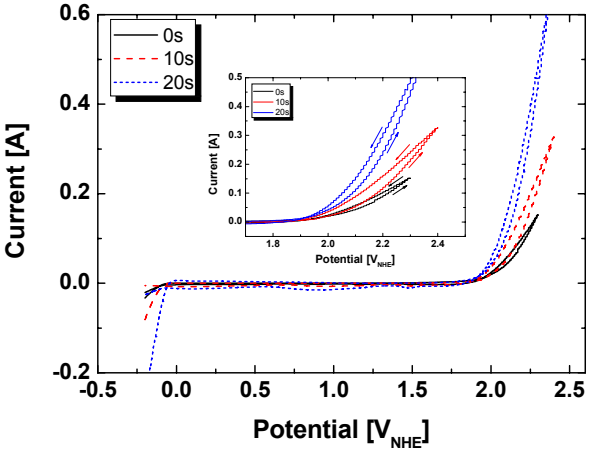

(a)

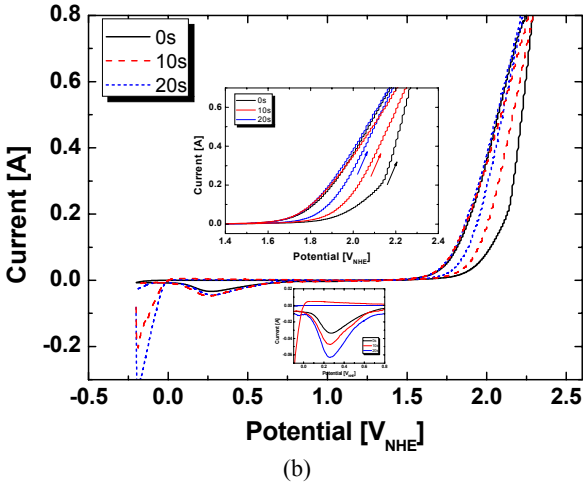

(b)

Fig. 3. Effect of electrodeposition time (0 ~ 20 s) for Pt nano deposits on the cyclic voltammograms of carbon electodes at (a) 25 ℃ and (b) 75 ℃, respectively.

increased abruptly after 1.9 V_{NHE}. The increase in anodic current density is attributed to both oxygen evolution reaction by the oxidation of water ($2H_2O \rightarrow O_2 + 4H^+ + 4e^-$) and carbon corrosion ($C + 2H_2O \rightarrow CO_2 + 4H^+ + 4e^-$). It is not easy to detect the independent contribution of carbon corrosion from the graph, because the oxygen evolution reaction and the carbon corrosion occur at similar potential range. Nevertheless, the fact that current did not decreased easily during reverse scan indicates that carbon corrosion which had initiated during forward scan was not repassivated. In addition, the anodic current for the carbon electrodes with Pt electrodeposits increased more sharply than that for the bare carbon electrode. This indicates that the overpotential for the charge transfer reaction is reduced by the catalytic action of Pt. Comparing two electrodes with Pt nano electrodeposits, the overpotential for the electrode electrodeposited for 20 s was lower than that for the electrode electrodeposited for 10 s.

At 75 ℃, the anodic current rise started at a potential of 200 mV lower than that at 25 ℃, indicating that electrochemical reactions including corrosion can be more activated at higher temperature. As in the case at 25 ℃, the larger the surface area of Pt electrodeposits, the lower the oxidation overpotential. In addition, differently from the cyclic voltammograms obtained at 25 ℃, a cathodic current peak appeared near at 0.3 V_{NHE} during reverse scan resulting from the oxygen reduction. During reverse scan, all three electrodes exhibited similar high current, indicating that the contribution of carbon corrosion became larger than that at 25 ℃. The carbon corrosion appears to stop completely below 1.6 V_{NHE}.

3.3 Current transients of the carbon electrodes at various applied potential

In order to investigate the effect of applied potential and electrodeposition time for Pt on the corrosion of carbon substrate, we measured the current transients of the electrodes as a function of time with applying the potentials of 1.8, 2.0, and 2.3 V at 25 ℃ and 1.6, 1.8, and 2.0 V at 75 ℃, respectively. In potential range where anodic current rise had increased, three potentials were selected from the cyclic voltammograms shown in Fig. 3. Fig. 4 shows the current transient curves of the electrodes at 25 ℃ and 75 ℃, respectively.

At 25 ℃ with an applied potential of 1.8 V_{NHE}, the anodic current for the carbon electrodes with and without Pt nano electrodeposits decreased gradually and finally stabilized with time. This suggests that carbon corrosion did not occur in these conditions. At 25 ℃ with an applied potential of 2.0 V_{NHE}, anodic current decreased sharply in the beginning and then increased gradually with time,

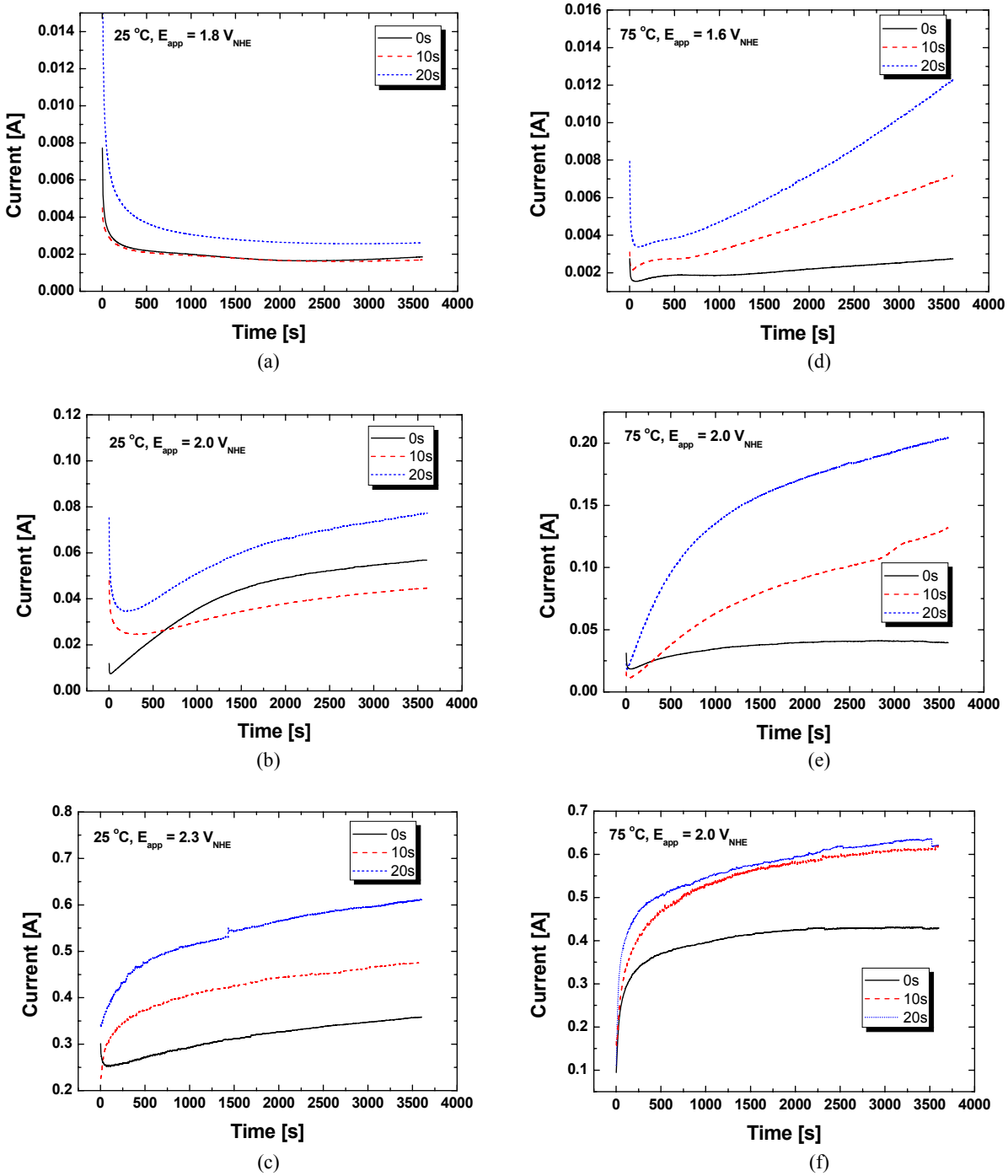

Fig. 4. Effect of applied potential on the current transient curves of carbon electrodes with and without Pt nano electrodeposits at 25 ℃ and 75 ℃, respectively.

indicating that the carbon corrosion propagated stably. At 2.3 V_{NHE}, the anodic current was much higher than that at other potentials due to the active propagation of carbon corrosion.

At 75 ℃, current transients were more active than those at 25 ℃. Even at 1.6 V_{NHE}, current increased gradually with time. As in the case at 25 ℃, the current for the carbon electrodes with Pt nano electrodeposits was higher than that for the bare carbon electrode.

Fig. 5 shows the power spectral density (PSD) plots converted from the current transients shown in Fig. 4 using maximum entropy method (MEM). The occurrence fre-

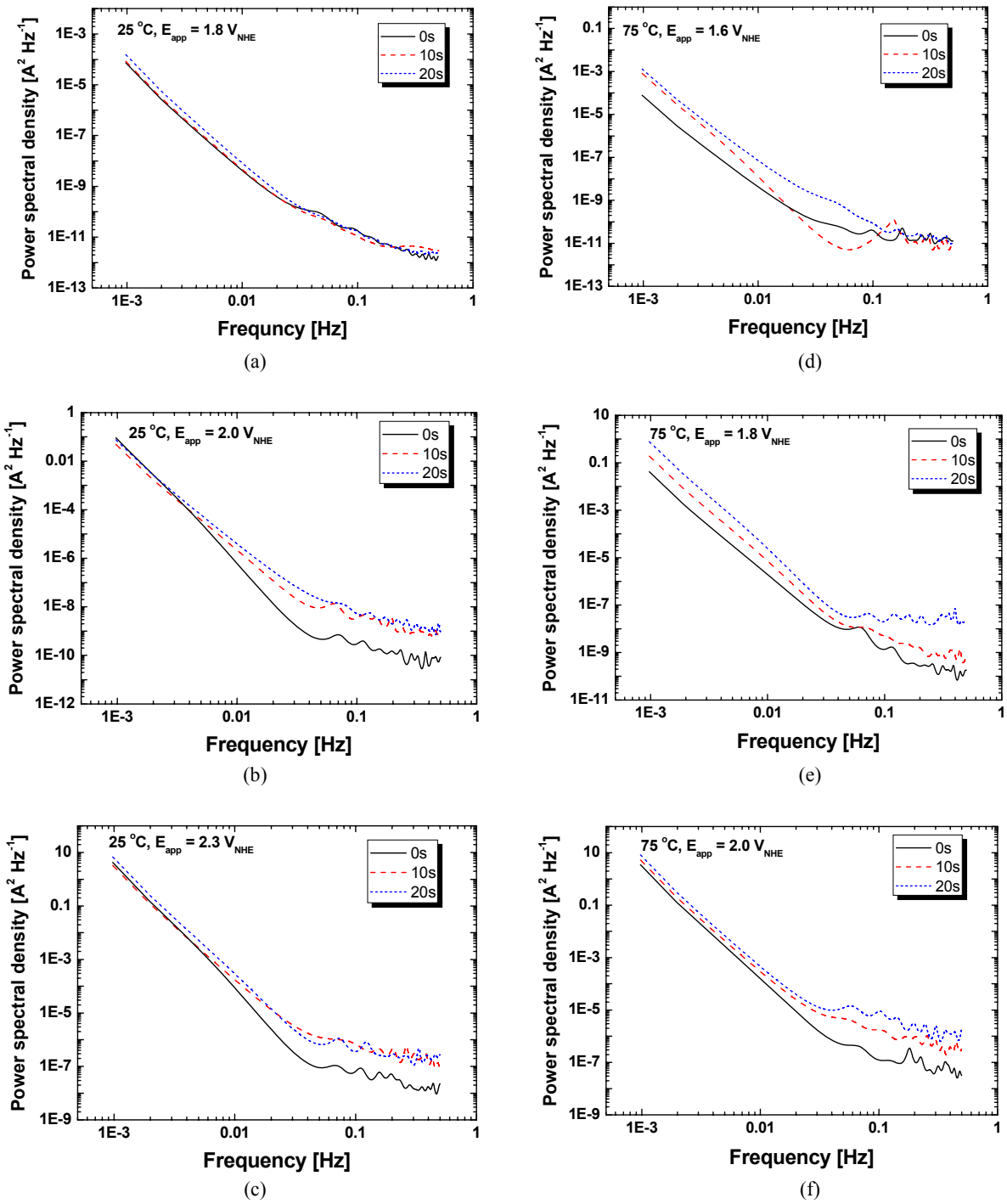

Fig. 5. Power spectral density plots transformed from the current transient curves.

quency and magnitude of current transients associated with the severity of carbon corrosion can be quantitatively analyzed using PSD, because not mean current but current fluctuation by electrochemical events such as corrosion is the main subject of investigation in this method. In particular, it is possible to separate the contribution of carbon corrosion from total anodic currents using this method. At 25 ℃ with the applied potential of 1.8 V_{NHE}, the shape of graphs for all three electrodes was similar, and the PSD decreased with frequency indicating that any characteristic electrochemical reactions such as corrosion did not occur. At 2.0 V_{NHE}, the PSD in high frequency region for the

carbon electrodes with Pt nano electrodeposits was higher than that for the bare carbon electrode. This result confirms that carbon corrosion is more active on the carbon electrodes with Pt nano electrodeposits than that on the bare carbon electrode. Furthermore, at 2.3 V_{NHE}, the PSD in overall frequency region for the carbon electrodes with Pt deposits was higher compared with that for the bare carbon electrode.

In addition, the PSD increased significantly with increasing temperature from 25 ℃ to 75 ℃. This phenomenon was more prominent for the carbon electrodes with Pt nano deposits. The current fluctuation is closely associated with the initiation and propagation of carbon corrosion. Thus, the carbon corrosion appears to be accelerated by Pt nano electrodeposits on carbon surface.

3.4 Corrosion behavior at Pt/C interface

Fig. 6 shows the surface morphologies of carbon electrodes after potentiostatic tests for 1h. The carbon electrodes were electrodeposited for 20 s before the potentiostatic tests. For the electrode exposed at 25 ℃ and 1.8 V_{NHE}, the surface of electrode does not appear to be damaged by corrosion. By contrast, for the electrode exposed at 2.0 V_{NHE}, the surrounding carbon substrate below a Pt nano particle collapsed, and the Pt particle sank. This phenomenon indicates that Pt nano electrodeposit accelerates the corrosion of surrounding carbon substrate. For the electrode exposed at 75 ℃ and 1.6 V_{NHE}, apparent change around Pt particle was not observed. However, on the whole the surface of carbon substrate appears to be roughened. For the electrode exposed at 1.8 V_{NHE}, Pt particles appear to lodge in the carbon substrate as in the case at 25 ℃. By contrast, Pt particles were not observed on surface of carbon electrodes exposed at higher potentials due to severe corrosion of the carbon substrate.

3.5 Electrode degradation by carbon corrosion in PEMFC

A PEMFC was also operated by repeating cycles. Fig. 7 shows the polarization curves and power density curves of PEMFC at different intervals. The initial maximum power density was 11 $W \cdot cm^{-2}$, which then decreases to 9.7 $W \cdot cm^{-2}$ after 255 cycle of operation. In addition, ac-

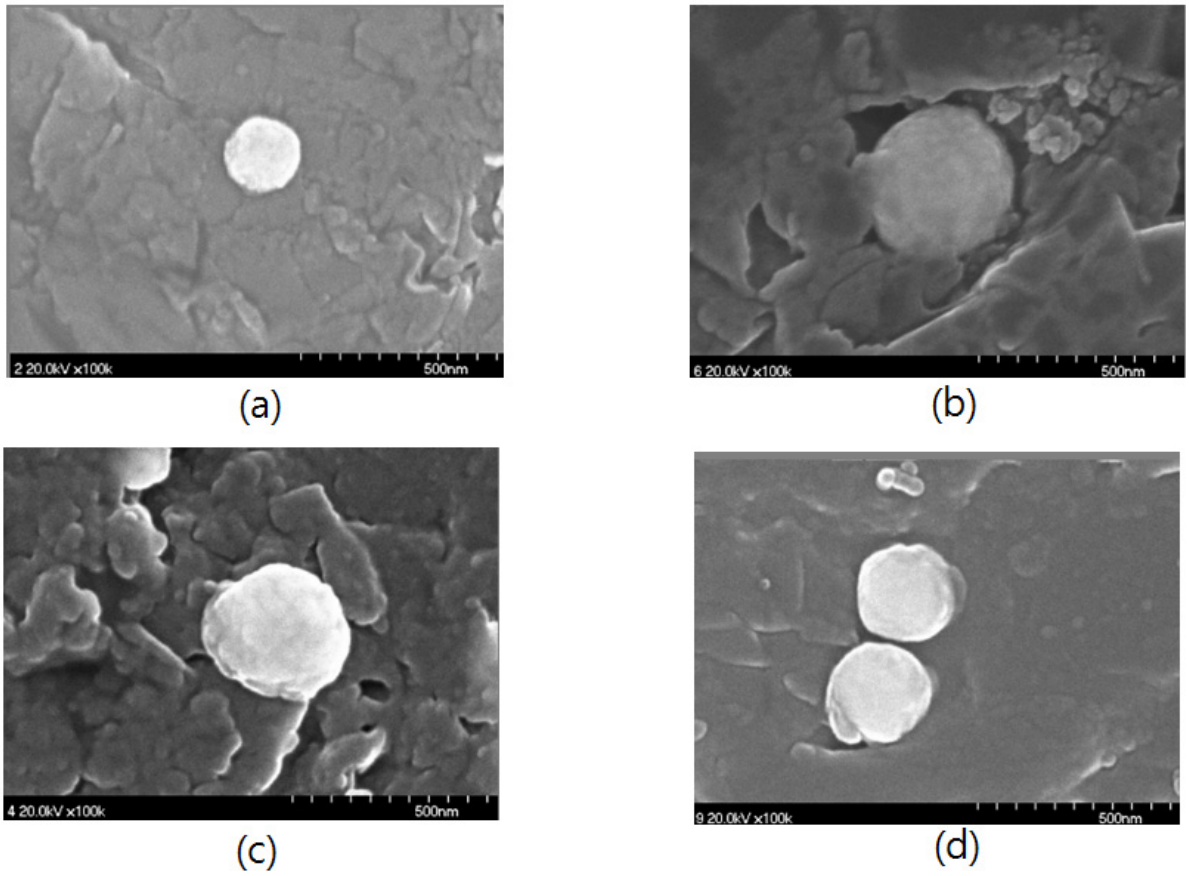

Fig. 6. Surface morphologies of the carbon electrodes, electrodeposited for 20s, after potentiostatic tests with applied potential of (a) 1.8 V_{NHE} and (b) 2.0 V_{NHE} at 25 ℃ and (c) 1.6 V_{NHE} and (d) 1.8 V_{NHE} at 75 ℃.

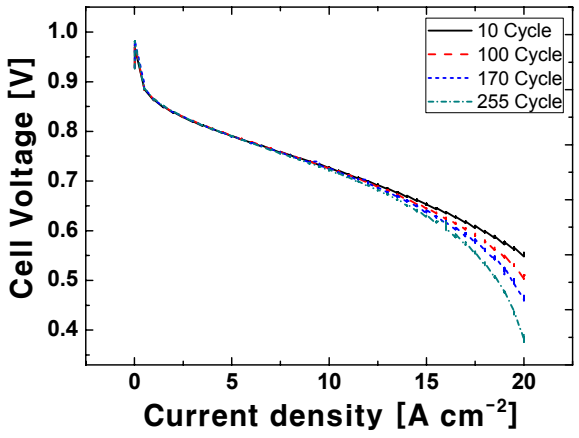

(a)

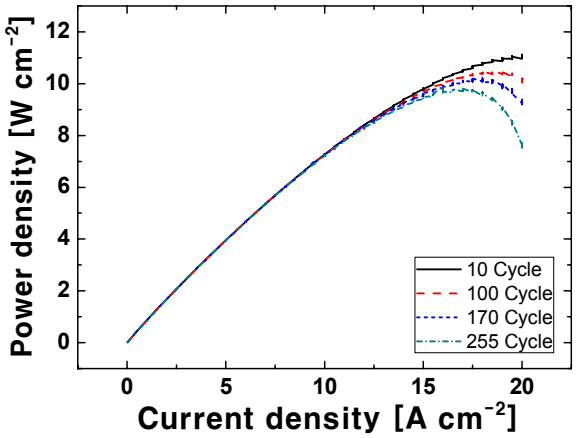

(b)

Fig. 7. Plots of the PEMFC testing cycles (a) polarization curves and (b) power density curves.

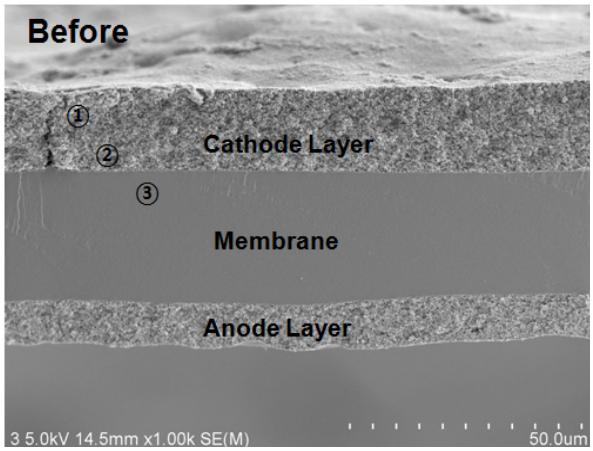

(a)

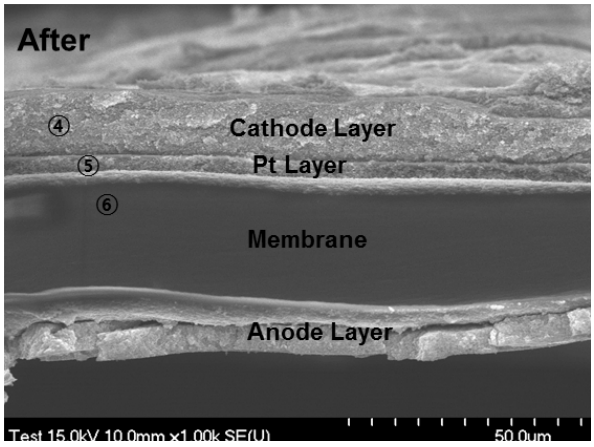

(b)

Fig. 8. Cross sectional view of MEA in a PEMFC (a) before and (b) after testing.

cording to the polarization curves, an increase in the experimental cycle decreased the cell voltage, particularly at high current densities. This degradation may be due to the deterioration of the oxygen reduction performance of the cathode catalyst. Furthermore, the increase in mass transfer resistance by the flooding in cathode part may degrade the performance with cycle.

After the test, the used MEA was cut, and its chemical compositions at different positions of its cross-section were analyzed by energy dispersive spectroscopy (EDS). Fig. 8 shows SEM images of the cross-section of MEA. Point analysis of the catalyst layer and membrane by EDS was carried out to analyze the chemical composition of Pt/C. Table 1 lists the composition of MEA before and after the test. The utilization feature of the catalyst can be observed from the results of point analysis. The catalyst closer to the membrane was used more in the reaction and Pt nano particles from the catalyst layer were easily dissolved. Furthermore, after operation for 255 cycle, a small amount of Pt particles was dissolved and diffused into the membrane.

Table 1. Point analysis by EDS of the membrane electrodes assembly (MEA) before and after the tests

Position	C	Pt	F
①	83.82	16.18	
②	85.67	14.33	
③	30.70		69.30
④	83.87	16.13	
⑤	82.34	17.66	
⑥	36.26		74.74

After the single cell test, the used MEA was separated and cut into smaller pieces for further analysis. XRD patterns of anode and cathode catalysts were recorded, as

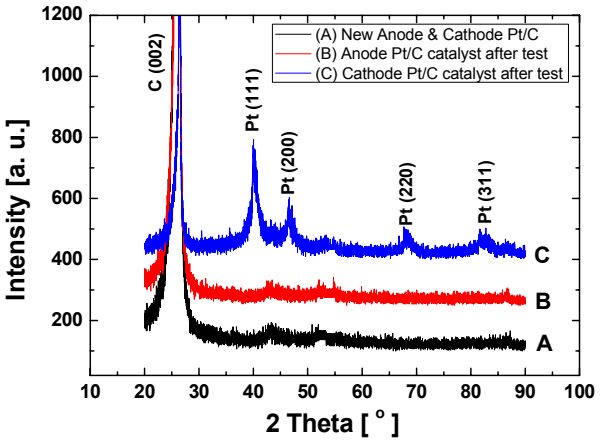

Fig. 9. Fig. 13. XRD pattern of MEA; (a) before test, (b) anode Pt/C catalyst layer after test and (c) cathode Pt/C layer after test.

shown in Fig. 9. The XRD pattern of new Pt/C catalyst is also shown for comparison. After the performance test, the Pt/C catalyst of the cathode exhibited a face-centered cubic (fcc) structure and major peaks of (111), (200), (220), and (311). However, the Pt/C catalyst of the anode does not show any Pt peaks. This confirms the dissolution of noble metal from the cathode layer and agglomeration at the interface of the cathode and membrane. Therefore, the Pt/C catalyst of the cathode was used more in the reaction and Pt nano particles from the catalyst layer were dissolved. In particular, the Pt enrichment at the interface indicates that the cathode was exposed to high potential at which carbon corrosion can occur. The enrichment of Pt in the membrane close to cathode layer was also reported by the previous research.[2)]

4. Conclusion

The density of the Pt electrodeposits on carbon substrate increased up to 20 s and then decreased to reduce surface energy, while the diameter of the electrodeposits increased gradually with increasing electodeposition time from 5 s to 30 s. The carbon electrodes with Pt nano electrodeposits exhibited the higher oxidation rate and lower oxidation overpotential compared with that of bare electrode. This phenomenon was more prominent at 75 ℃ than 25 ℃. In addition, the current transients and the corresponding PSD of the carbon electrodes with Pt nano electrodeposits were much higher than those of the base electrode. The carbon corrosion at Pt/C interface appears to be highly accelerated by Pt nano electrodeposits. Furthermore, the polarization and power density curves of PEMFC showed degradation in the performance due to a deterioration of cathode catalyst material and Pt dissolution, which was further conformed by EDS and XRD analysis of MEA after the test.

Acknowledgment

This work was supported by the Korea Research Foundation Grant (MOEHRD, Basic Research Fund)(KRF-2007-313-D00950) and by Basic Research Laboratories (BRL) Program of National Research Foundation of Korea (2009-0085441).

References

1. Z. Siroma, K. Ishii, K. Yasuda, Y. Miyazaki, M. Inaba, and A. Tasaka, *Electrochem. Commun.*, **7**, 1153 (2005).
2. J. P. Meyers and R. M. Darling, *J. Electrochem. Soc.*, **153**, A1432 (2006).
3. M. M. E. Duarte, A. S. Pilla, J. M. Sieben, and C. E. Mayer, *Electrochem. Commun.*, **8**, 159 (2006).
4. M. S. Suh, C. J. Park, and H. S. Kwon, *Surf. Coat. Tech.*, **200**, 3527 (2006).
5. C. J. Park and H. S. Kwon, *Mater. Chem. Phys.*, **91**, 355 (2005).
6. J. M. Han, *Corros. Sci. Tech.*, **8**, 203 (2009).
7. D. S. Seo, K. H. Lee, and H. S. Kim, *Corros. Sci. Tech.*, **7**, 319 (2008).